A Review of the Modal Decomposition Matrix for Calculating the Far Field of an Infinitely Flanged Rectangular Waveguide

Gregory A. Mitchell [1] and Wasyl Wasykiwskyj [2]

[1] U.S. Army Research Laboratory
Adelphi, MD 20783, USA
gregory.a.mitchell1.civ@mail.mil

[2] Department of Electrical and Computer Engineering
The George Washington University, Washington, DC 20052, USA
wasylkiw@gwu.edu

Abstract ─ We determine the radiation from an infinitely flanged rectangular waveguide using the modal decomposition matrix (MDM) method. The MDM method computes the electromagnetic field components at the aperture in the Fourier domain by representing the radiated field in terms of a sampling of the free-space transverse wave number. The results of the MDM approach show good agreement with numerical approaches using commercial electromagnetic modeling software.

Index Terms ─ EM propagation, flanged rectangular waveguide, modal decomposition matrix, spherical value decomposition, stationary phase.

I. INTRODUCTION

In practice, designers use flush mounted aperture antennas widely and approximate their models by an aperture in an infinite conducting surface (infinite flange). The analysis of radiation from an infinitely flanged open rectangular waveguide has been widely studied and presenting using different analytical methods for calculating the electromagnetic (EM) fields at the aperture [1-3]. Furthermore, the solutions determined by these methods reasonably approximate those of a radiating waveguide with a finite flange [4]. After calculating the EM fields at the aperture, the stationary phase equation determines the radiated far field [5]. Although accurate, known methods require the additional calculation of the Fourier transform of the EM fields at the aperture before they can apply them to the stationary phase equation. In high fidelity computer simulations with many millions of mesh cells, algorithms numerically compute the EM fields at the boundaries of every mesh cell across the waveguide aperture. For far field calculations using stationary phase, these methods also require a Fourier transform of every EM field at the boundary of every mesh cell across the aperture leading to unnecessary additional computational expense.

This paper reviews a less computationally costly approach that analytically computes the components of the EM fields at the aperture of an infinitely flanged open rectangular waveguide in the Fourier domain. Our approach directly solves for these fields without the need of a computationally expensive Fourier transform. The approach uses the modal decomposition matrix (MDM) based on a modal sampling of the transverse free space wave number. This approach results in a matrix equation solving directly for the Fourier field components needed for stationary phase calculations of the radiated far fields. The authors originally published the MDM method as an internal report [6], and mean for this review paper to distribute the results to a wider audience of peer reviewed journals.

We compare the results determined by the MDM method to the far field radiation patterns and return loss calculations achieved by CST Studio Suite 2017 for a 3D model and simulation of the same problem. The comparison shows excellent agreement between the simulations and the numerical techniques using the MDM method.

II. MODAL DECOMPOSITION OF A RECTANGULAR WAVEGUIDE

This section describes the theory of matching the transverse electric (TE) and magnetic (TM) fields that exist inside a uniform rectangular waveguide to those of the radiated far fields in free space. We base the below description of the modal decomposition on known theory [7, 8]. We assume the dominant propagating mode generates the transverse EM fields inside the waveguide. The cutoff frequency (f_c) of the waveguide determines when the dominant mode changes from an attenuating to a propagating mode. For a rectangular waveguide, the dominant mode is TE_{10} [9].

By matching to the spectral component of the

Submitted On: December 19, 2017
Accepted On: November 12, 2018

1054-4887 © ACES

radiated field at the aperture, we derive a system of equations that yield the transverse aperture EM fields in the Fourier domain. Based on this we use the stationary phase equation to calculate the far field radiation patterns. We now construct the form of the electric and magnetic fields that exist inside the waveguide due to a propagating TE_{10} mode.

A. Propagating TE_{10} mode case

We assume the incident TE_{10} wave in Fig. 1 exists in the waveguide with the following form:

$$\underline{E}_{Tinc}(\underline{r}) = \underline{e}''_N(\underline{\rho})V(z), \tag{1}$$

$$\underline{H}_{Tinc}(\underline{r}) = \underline{h}''_N(\underline{\rho})I(z), \tag{2}$$

where $\underline{r} = x\cdot\underline{x}_o + y\cdot\underline{y}_o + z\cdot\underline{z}_o$, $\underline{\rho} = x\cdot\underline{x}_o + y\cdot\underline{y}_o$, and $V(z)$ and $I(z)$ are the voltage and current at point z inside the waveguide. N denotes that the incident mode is propagating in the waveguide and '' denotes a TE mode while ' denotes a transverse magnetic (TM) mode.

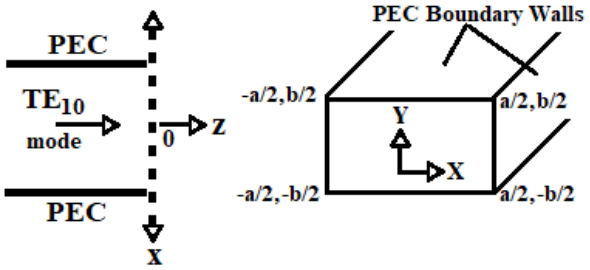

Fig. 1. Illustration of the boundary between the waveguide and free space at z=0 and its transverse cross section.

Figure 1 shows two orientations of the same rectangular waveguide. A half space boundary exists at z=0, and the waveguide extends to -∞ in the $\underline{z}_o$-direction. The literature describes this as the semi-infinite waveguide approximation [7].

We define the mode functions $\underline{e}_\upsilon(\underline{\rho})$ and $\underline{h}_\upsilon(\underline{\rho})$:

$$\underline{e}'_\upsilon(\underline{\rho}) = \nabla_T \Phi_\upsilon(\underline{\rho})/(\pi A'_\upsilon) = \left[\underline{x}_o \frac{m}{a}\cos\left(\frac{m\pi}{a}\left(x+\frac{a}{2}\right)\right)\sin\left(\frac{n\pi}{b}\left(y+\frac{b}{2}\right)\right), \right. \tag{3}$$
$$\left. +\underline{y}_o \frac{n}{b}\sin\left(\frac{m\pi}{a}\left(x+\frac{a}{2}\right)\right)\cos\left(\frac{n\pi}{b}\left(y+\frac{b}{2}\right)\right)\right]$$

$$\underline{h}'_\upsilon(\underline{\rho}) = \underline{z}_o \times \underline{e}'_\upsilon(\underline{\rho})/(\pi A'_\upsilon) = \left[\underline{x}_o \frac{n}{b}\sin\left(\frac{m\pi}{a}\left(x+\frac{a}{2}\right)\right)\cos\left(\frac{n\pi}{b}\left(y+\frac{b}{2}\right)\right), \right. \tag{4}$$
$$\left. -\underline{y}_o \frac{m}{a}\cos\left(\frac{m\pi}{a}\left(x+\frac{a}{2}\right)\right)\sin\left(\frac{n\pi}{b}\left(y+\frac{b}{2}\right)\right)\right]$$

$$\underline{e}''_\upsilon(\underline{\rho}) = \underline{z}_o \times \underline{h}''_\upsilon(\underline{\rho})/(\pi A''_\upsilon) = \left[\underline{x}_o \frac{n}{b}\cos\left(\frac{m\pi}{a}\left(x+\frac{a}{2}\right)\right)\sin\left(\frac{n\pi}{b}\left(y+\frac{b}{2}\right)\right), \right. \tag{5}$$
$$\left. -\underline{y}_o \frac{m}{a}\sin\left(\frac{m\pi}{a}\left(x+\frac{a}{2}\right)\right)\cos\left(\frac{n\pi}{b}\left(y+\frac{b}{2}\right)\right)\right]$$

$$\underline{h}''_\upsilon(\underline{\rho}) = -\nabla_T \Psi_\upsilon(\underline{\rho})/(\pi A''_\upsilon) = \left[\underline{x}_o \frac{m}{a}\sin\left(\frac{m\pi}{a}\left(x+\frac{a}{2}\right)\right)\cos\left(\frac{n\pi}{b}\left(y+\frac{b}{2}\right)\right), \right. \tag{6}$$
$$\left. +\underline{y}_o \frac{n}{b}\cos\left(\frac{m\pi}{a}\left(x+\frac{a}{2}\right)\right)\sin\left(\frac{n\pi}{b}\left(y+\frac{b}{2}\right)\right)\right]$$

where υ represents the *(m, n)* pair known as the mode number where $(m, n)\geq 0$. In the remainder of this paper, we use $\upsilon=M$ or N to denote non-incident and incident modes in the waveguide, but these also represent *(m, n)* pairs. For instance, the TE_{10} mode has mode indices of m=1 and n=0. We determine A'_υ and A''_υ by normalizing (3-6) across the transverse plane of the waveguide:

$$A'^{2}_{mn}\int_{-\frac{b}{2}}^{\frac{b}{2}}\int_{-\frac{a}{2}}^{\frac{a}{2}} \underline{e}'_{mn}(\underline{\rho})\bullet\underline{e}'_{kl}(\underline{\rho})dxdy = \delta_{mk}\delta_{nl}, \tag{7}$$

$$A''^{2}_{mn}\int_{-\frac{b}{2}}^{\frac{b}{2}}\int_{-\frac{a}{2}}^{\frac{a}{2}} \underline{e}''_{mn}(\underline{\rho})\bullet\underline{e}''_{kl}(\underline{\rho})dxdy = \delta_{mk}\delta_{nl}, \tag{8}$$

where δ_{mk} is defined as δ_{mk}=0 for $m\neq k$, δ_{mm}=1 and similarly for δ_{nl}. Solving (8, 9) for the normalization constants yield:

$$A'_{mn} = \left(\frac{2}{\pi}\right)\frac{P_{mn}}{\sqrt{m^2\frac{a}{b}+n^2\frac{b}{a}}}, \tag{9}$$

$$A''_{mn} = \left(\frac{\sqrt{\xi_m\xi_n}}{\pi}\right)\frac{P_{mn}}{\sqrt{m^2\frac{b}{a}+n^2\frac{a}{b}}}, \tag{10}$$

$$\xi_m, \xi_n = \begin{cases}1; & m,n=0\\ 2; & m,n\geq 1\end{cases}$$

where P_{mn} is the propagating mode's amplitude.

Taking (3-6) and (9, 10) into account we construct the total transverse fields inside the waveguide for $z\leq 0$:

$$\underline{E}_T(\underline{r}) = \underline{e}''_N(\underline{\rho})\left(e^{-j\kappa''_N z}+\Gamma''_N(z)e^{+j\kappa''_N z}\right) + \sum_{M\neq N}\left[\Gamma'_M(z)\underline{e}'_M(\underline{\rho})e^{+j\kappa'_M z}\right., \tag{11}$$
$$\left.+\Gamma''_M(z)\underline{e}''_M(\underline{\rho})e^{+j\kappa''_M z}\right]$$

$$\underline{H}_T(\underline{r}) = \frac{\underline{h}''_N(\underline{\rho})}{Z''_N}\left(e^{-j\kappa''_N z} - \Gamma''_N(z)\, e^{+j\kappa''_N z}\right) - \sum_{M\neq N}\left[\frac{\Gamma'_M\ \underline{h}'_M(\underline{\rho}) e^{+j\kappa'_M z}}{Z'_M} + \frac{\Gamma''_M\ \underline{h}''_M(\underline{\rho}) e^{+j\kappa''_M z}}{Z''_M}\right], \quad (12)$$

where Γ_υ is the reflection coefficient at the aperture. We define Z'_υ, Z''_υ, and κ_υ as:

$$Z'_\upsilon = \frac{\kappa_\upsilon}{\omega\varepsilon}, \quad (13)$$

$$Z''_\upsilon = \frac{\omega\mu}{\kappa_\upsilon}, \quad (14)$$

$$\kappa_\upsilon = \sqrt{k_o^2 - \left(\frac{m\pi}{a}\right)^2 + \left(\frac{n\pi}{b}\right)^2}. \quad (15)$$

Here k_o is the free space wave number, $(m\pi/a)^2 = k_x^2$, and $(n\pi/b)^2 = k_y^2$. We define the equations for the transverse radiated electric and magnetic fields when $z \geq 0$:

$$\underline{E}_T(\underline{r}) = \frac{1}{(2\pi)^2}\int_{-\infty}^{\infty}\int_{-\infty}^{\infty}\tilde{\underline{E}}_{T\upsilon}(k_{T\upsilon}) e^{-j\underline{k}\cdot\underline{r}} dk_x dk_y, \quad (16)$$

$$\underline{H}_T(\underline{r}) = \frac{1}{(2\pi)^2}\int_{-\infty}^{\infty}\int_{-\infty}^{\infty}\tilde{\underline{H}}_{T\upsilon}(k_{T\upsilon}) e^{-j\underline{k}\cdot\underline{r}} dk_x dk_y, \quad (17)$$

where $k_{T\upsilon}$ represents the mode dependent (k_x, k_y) pair and ~ denotes these components are in the Fourier domain.

III. MODAL DECOMPOSITION MATRIX METHOD

We now equate the vector equations of $\underline{E}_T(\underline{r})$ and $\underline{H}_T(\underline{r})$ of (11, 12) to (16, 17). Doing so equates the TE and TM fields at the waveguide free space boundary of $z=0$ in Fig. 1. The expressions obtained populate the MDM allowing us to solve for the Fourier components of the transverse fields at the aperture of the open waveguide.

A. Derivation of MDM equation

To express the fields at the waveguide free space boundary we equate (11) to (16) and (12) to (17). Setting $z=0$ yields:

$$(1+\Gamma''_N)\underline{e}''_N(\underline{\rho}) + \sum_{M\neq N}\left[\Gamma'_M\ \underline{e}'_M(\underline{\rho}) + \Gamma''_M\ \underline{e}''_M(\underline{\rho})\right] = \frac{1}{(2\pi)^2}\int_{-\infty}^{+\infty}\int_{-\infty}^{+\infty}\tilde{\underline{E}}_{T\upsilon}(k_{T\upsilon}) e^{-j\underline{k}_T\bullet\underline{\rho}} dk_x dk_y, \quad (18)$$

$$(1-\Gamma''_N)\frac{\underline{h}''_N(\underline{\rho})}{Z''_N} - \sum_{M\neq N}\left[\Gamma'_M\ \frac{\underline{h}'_M(\underline{\rho})}{Z'_M} + \Gamma''_M\ \frac{\underline{h}''_M(\underline{\rho})}{Z''_M}\right] = \frac{1}{(2\pi)^2}\int_{-\infty}^{+\infty}\int_{-\infty}^{+\infty}\tilde{\underline{H}}_{T\upsilon}(k_{T\upsilon}) e^{-j\underline{k}_T\bullet\underline{\rho}} dk_x dk_y, \quad (19)$$

The following orthogonality equations [6]:

$$\iint_S \underline{e}_k(\underline{\rho})\bullet\underline{e}_l(\underline{\rho})dxdy = \delta_{kl}, \quad (20)$$

$$\iint_S \underline{h}_k(\underline{\rho})\bullet\underline{h}_l(\underline{\rho})dxdy = \delta_{kl}, \quad (21)$$

allow us to simplify (18, 19) in terms of Γ_υ, $\tilde{\underline{E}}(k_x, k_y)$, and $\tilde{\underline{H}}(k_x, k_y)$, where S is the surface dimensions of the rectangular waveguide. By limiting the bounds of integration in (20, 21), we enforce the boundary condition that $\underline{E}_T(\underline{r}) = 0$ on the conducting surface of the waveguide and flange. Using the following substitutions:

$$\hat{\underline{\alpha}}_\upsilon(k_{T\upsilon}) = \iint_S \frac{e^{-j\underline{\kappa}_{T\upsilon}\bullet\underline{\rho}}}{(2\pi)^2}\underline{\alpha}_\upsilon(\underline{\rho})dxdy, \quad (22)$$

$$\iint_S\left[\hat{\underline{t}}_\upsilon(k_{T\upsilon})\bullet\tilde{\underline{T}}_{T\upsilon}(k_{T\upsilon})\right]dk_x dk_y = \left[\hat{\underline{t}}_\upsilon(k_{T\upsilon}),\ \tilde{\underline{T}}_{T\upsilon}(k_{T\upsilon})\right], \quad (23)$$

we can rewrite (18, 19) as the following system of equations:

$$(1+\Gamma''_N) = \left[\hat{\underline{e}}''_N(k_{TN}),\ \tilde{\underline{E}}_{TN}(k_{TN})\right], \quad (24)$$

$$(1-\Gamma''_N) = Z''_N\left[\hat{\underline{h}}''_N(k_{TN}),\ \tilde{\underline{H}}_{TN}(k_{TN})\right], \quad (25)$$

$$\Gamma''_M = \left[\hat{\underline{e}}''_M(k_{TM}),\ \tilde{\underline{E}}_{TM}(k_{TM})\right], \quad (26)$$

$$\Gamma''_M = -Z''_M\left[\hat{\underline{h}}''_M(k_{TM}),\ \tilde{\underline{H}}_{TM}(k_{TM})\right], \quad (27)$$

$$(1+\Gamma'_N) = \left[\hat{\underline{e}}'_N(k_{TN}),\ \tilde{\underline{E}}_{TN}(k_{TN})\right], \quad (28)$$

$$(1-\Gamma'_N) = Z'_N\left[\hat{\underline{h}}'_N(k_{TN}),\ \tilde{\underline{H}}_{TN}(k_{TN})\right], \quad (29)$$

$$\Gamma'_M = \left[\hat{\underline{e}}'_M(k_{TM}),\ \tilde{\underline{E}}_{TM}(k_{TM})\right], \quad (30)$$

$$\Gamma'_M = -Z'_M\left[\hat{\underline{h}}'_M(k_{TM}),\ \tilde{\underline{H}}_{TM}(k_{TM})\right], \quad (31)$$

We use equations (24-31) to populate the MDM and solve for the Fourier components of the fields at the aperture. By adding like Γ_υ terms together from (24-31) we rewrite the system of equations as:

$$\left[\hat{\underline{e}}''_\upsilon(k_{T\upsilon}),\ \tilde{\underline{E}}_T(k_{T\upsilon})\right] + Z''_\upsilon\left[\hat{\underline{h}}''_\upsilon(k_{T\upsilon}),\ \tilde{\underline{H}}_{T\upsilon}(k_{T\upsilon})\right] = 2\delta_{\upsilon N}, \quad (32)$$

$$\left[\hat{\underline{e}}'_\upsilon(k_{T\upsilon}),\ \tilde{\underline{E}}_T(k_{T\upsilon})\right] + Z'_\upsilon\left[\hat{\underline{h}}'_\upsilon(k_{T\upsilon}),\ \tilde{\underline{H}}_{T\upsilon}(k_{T\upsilon})\right] = 2\delta_{\upsilon N}. \quad (33)$$

By representing the integrals in k space as a Riemann Sum over k_x and k_y, we will formulate the MDM equation. Simplifying (32, 33), we write $\tilde{\underline{H}}_{T\upsilon}(k_{T\upsilon})$ in terms of $\tilde{\underline{E}}_{T\upsilon}(k_{T\upsilon})$ leaving a single unknown. Starting with the expression:

$$\tilde{\underline{H}}_{T\upsilon}(k_x,k_y) = \frac{1}{\omega\mu_o}\left[\left(\underline{z}_o\times\tilde{\underline{E}}_{T\upsilon}(k_{T\upsilon})\right)k_{z\upsilon} - \left(\frac{\underline{k}_{T\upsilon}\times\underline{z}_o}{k_{z\upsilon}}\right)\left(\underline{k}_{T\upsilon}\bullet\tilde{\underline{E}}_{T\upsilon}(k_{T\upsilon})\right)\right], \quad (34)$$

we form the matrix equation:

$$\tilde{\underline{H}}_{T\upsilon}(k_{T\upsilon}) = \begin{bmatrix}\tilde{\underline{H}}_{x\upsilon}(k_{T\upsilon})\\ \tilde{\underline{H}}_{y\upsilon}(k_{T\upsilon})\end{bmatrix} = \underline{\underline{A}}\bullet\tilde{\underline{E}}_{T\upsilon}(k_{T\upsilon}) = \begin{bmatrix}\underline{\underline{A}}_{xx} & \underline{\underline{A}}_{xy}\\ \underline{\underline{A}}_{yx} & \underline{\underline{A}}_{yy}\end{bmatrix}\begin{bmatrix}\tilde{\underline{E}}_{x\upsilon}(k_{T\upsilon})\\ \tilde{\underline{E}}_{y\upsilon}(k_{T\upsilon})\end{bmatrix}. \quad (35)$$

We solve for $\underline{\underline{A}}$ by expanding (33) as:

$$\underline{\underline{A}}\bullet\tilde{\underline{E}}_{T\upsilon} = \tilde{\underline{H}}_{T\upsilon} = \frac{\underline{\underline{K}}_\upsilon}{\omega\mu_o\kappa_\upsilon}\bullet\tilde{\underline{E}}_{T\upsilon}, \quad (36)$$

$$\underline{\underline{K}}_\upsilon = \begin{bmatrix}-k_xk_y & -\left(k_o^2-k_x^2\right)\\ k_o^2-k_y^2 & k_xk_y\end{bmatrix}, \quad (37)$$

where k_x and k_y are mode number dependent.

Equations (36, 37) are a shorthand notation representing the system of equations that construct our MDM equation. However, longhand notation will better demonstrate how (36) maps to a system of equations. We express (36) by a set of two the Riemann sums over k_x and k_y:

$$\sum_{k_y}\sum_{k_x}\left[\left(\hat{\underline{e}}''_\upsilon(k_{T\upsilon}) + Z''_\upsilon\,\underline{\underline{A}}\bullet\hat{\underline{h}}''_\upsilon(k_{T\upsilon})\right)\bullet\tilde{\underline{E}}_{T\upsilon}(k_{T\upsilon})\right]\Delta k_x\Delta k_y = \delta_{\upsilon N}, \quad (38)$$

$$\sum_{k_y}\sum_{k_x}\left[\left(\hat{\underline{e}}'_\upsilon(k_{T\upsilon}) + Z'_\upsilon\,\underline{\underline{A}}\bullet\hat{\underline{h}}'_\upsilon(k_{T\upsilon})\right)\bullet\tilde{\underline{E}}_{T\upsilon}(k_{T\upsilon})\right]\Delta k_x\Delta k_y = \delta_{\upsilon N}. \quad (39)$$

We can now write the MDM from (38, 39) to solve directly for $\tilde{\underline{E}}_{T\upsilon}$ with no need to invoke a Fourier transform. In doing so, each value of υ represents a different waveguide mode corresponding to the MDM row index. Each value of υ also represents a discrete index of k_x and k_y corresponding to the MDM column index. This creates a square matrix with a total of L samples of k_x and k_y as well as L modes.

Note from (22) that $\underline{\alpha}_\upsilon(\underline{\rho})$ still includes an $\underline{x}_o$ and $\underline{y}_o$ vector dependence. If we let,

$$M''_{\upsilon x}(k_{T\upsilon}) = \left[\left(\hat{\underline{e}}''_\upsilon(k_{T\upsilon}) + Z''_\upsilon\,\underline{\underline{A}}\bullet\hat{\underline{h}}''_\upsilon(k_{T\upsilon})\right)\bullet\tilde{\underline{E}}_{T\upsilon}(k_{T\upsilon})\right]\bullet\underline{x}_o, \quad (40)$$

$$M''_{\upsilon Y}(k_{T\upsilon}) = \left[\left(\hat{\underline{e}}''_\upsilon(k_{T\upsilon}) + Z''_\upsilon\,\underline{\underline{A}}\bullet\hat{\underline{h}}''_\upsilon(k_{T\upsilon})\right)\bullet\tilde{\underline{E}}_{T\upsilon}(k_{T\upsilon})\right]\bullet\underline{y}_o, \quad (41)$$

$$M'_{\upsilon x}(k_{T\upsilon}) = \left[\left(\hat{\underline{e}}'_\upsilon(k_{T\upsilon}) + Z'_\upsilon\,\underline{\underline{A}}\bullet\hat{\underline{h}}'_\upsilon(k_{T\upsilon})\right)\bullet\tilde{\underline{E}}_{T\upsilon}(k_{T\upsilon})\right]\bullet\underline{x}_o, \quad (42)$$

$$M'_{\upsilon Y}(k_{T\upsilon}) = \left[\left(\hat{\underline{e}}'_\upsilon(k_{T\upsilon}) + Z'_\upsilon\,\underline{\underline{A}}\bullet\hat{\underline{h}}'_\upsilon(k_{T\upsilon})\right)\bullet\tilde{\underline{E}}_{T\upsilon}(k_{T\upsilon})\right]\bullet\underline{y}_o, \quad (43)$$

then we populate the MDM equation using (40-43) and a matrix of four LxL quadrants:

$$\begin{bmatrix}\underline{\underline{M}}''_{\upsilon X} & \underline{\underline{M}}''_{\upsilon Y}\\ \underline{\underline{M}}'_{\upsilon X} & \underline{\underline{M}}'_{\upsilon Y}\end{bmatrix}\bullet\begin{bmatrix}\tilde{\underline{E}}_x(k_{T\upsilon})\\ \tilde{\underline{E}}_y(k_{T\upsilon})\end{bmatrix} = \begin{bmatrix}2\underline{\delta}''_{\upsilon N}\\ 2\underline{\delta}'_{\upsilon N}\end{bmatrix}, \quad (44)$$

$$\underline{\underline{M}}''_{\upsilon X} = \begin{bmatrix}M''_{1x}(k_{T1}) & \cdots & M''_{1x}(k_{TL})\\ \vdots & \ddots & \vdots\\ M''_{Lx}(k_{T1}) & \cdots & M''_{Lx}(k_{TL})\end{bmatrix}, \quad (45)$$

$$\underline{\underline{M}}''_{\upsilon Y} = \begin{bmatrix}M''_{1y}(k_{T1}) & \cdots & M''_{1y}(k_{TL})\\ \vdots & \ddots & \vdots\\ M''_{Ly}(k_{T1}) & \cdots & M''_{Ly}(k_{TL})\end{bmatrix}, \quad (46)$$

$$\underline{\underline{M}}'_{\upsilon X} = \begin{bmatrix} M'_{1x}(k_{T1}) & \cdots & M'_{1x}(k_{TL}) \\ \vdots & \ddots & \vdots \\ M'_{Lx}(k_{T1}) & \cdots & M'_{Lx}(k_{TL}) \end{bmatrix}, \quad (47)$$

$$\underline{\underline{M}}'_{\upsilon Y} = \begin{bmatrix} M'_{1y}(k_{T1}) & \cdots & M'_{1y}(k_{TL}) \\ \vdots & \ddots & \vdots \\ M'_{Ly}(k_{T1}) & \cdots & M'_{Ly}(k_{TL}) \end{bmatrix}, \quad (48)$$

$$\underline{\tilde{E}}_{x\upsilon}(k_{T\upsilon}) = \begin{bmatrix} \tilde{E}_{x1}(k_{T1}) & \cdots & \tilde{E}_{xL}(k_{TL}) \end{bmatrix}^T, \quad (49)$$

$$\underline{\tilde{E}}_{y\upsilon}(k_{T\upsilon}) = \begin{bmatrix} \tilde{E}_{y1}(k_{T1}) & \cdots & \tilde{E}_{yL}(k_{TL}) \end{bmatrix}^T, \quad (50)$$

$$2\underline{\delta}''_{\upsilon N} = \begin{bmatrix} 2 & 0 & \cdots & 0 \end{bmatrix}^T, \quad (51)$$

$$2\underline{\delta}'_{\upsilon N} = \begin{bmatrix} 0 & 0 & \cdots & 0 \end{bmatrix}^T. \quad (52)$$

Quadrant $\underline{\underline{M}}''_{\upsilon X}$ corresponds to elements that represent TE modes in the $\underline{x}_o$ direction, quadrant $\underline{\underline{M}}''_{\upsilon Y}$ corresponds to elements that represent TE modes in the $\underline{y}_o$ direction, quadrant $\underline{\underline{M}}'_{\upsilon X}$ corresponds to elements representing TM modes in the $\underline{x}_o$ direction, and quadrant $\underline{\underline{M}}'_{\upsilon Y}$ corresponds to elements representing TM modes in the $\underline{y}_o$ direction. We separate the $\underline{x}_o$ components and $\underline{y}_o$ components to obtain individual solutions to $\underline{\tilde{E}}_{x\upsilon}(k_{T\upsilon})$ and $\underline{\tilde{E}}_{y\upsilon}(k_{T\upsilon})$ at z=0. Each MDM quadrant is LxL in dimension yielding a 2Lx2L matrix. The solutions to $\underline{\tilde{E}}_{x\upsilon}(k_{T\upsilon})$ and $\underline{\tilde{E}}_{y\upsilon}(k_{T\upsilon})$ are size L column vectors. The right hand side column vector of equation (44) is zero except for the first element that corresponds to the propagating TE_{10} mode.

As with any numerical approximation to a continuous function, L must be large enough to ensure an accurate representation of the original function. However, a large L necessitates using many weak attenuating modes in the MDM equation. This leads to a singular matrix, which is not invertible. Therefore, in solving (44) we must use singular value decomposition (SVD) to determine the inverse of the MDM [10].

When using the SVD method the number of singular values used to generate the inverse of the MDM in (44) plays a crucial role. A matrix with dimensions 2Lx2L will have 2L singular values. Many of the singular values will have magnitudes approaching zero. The calculation should not use these values or they will skew the accuracy of the numerical results. On the other hand, if you have multiple singular values with large magnitudes then eliminating any of them will also skew the results. Figure 2 shows the singular values in descending order for a 24-mode MDM calculation. The number of singular values used for this particular calculation is 5.

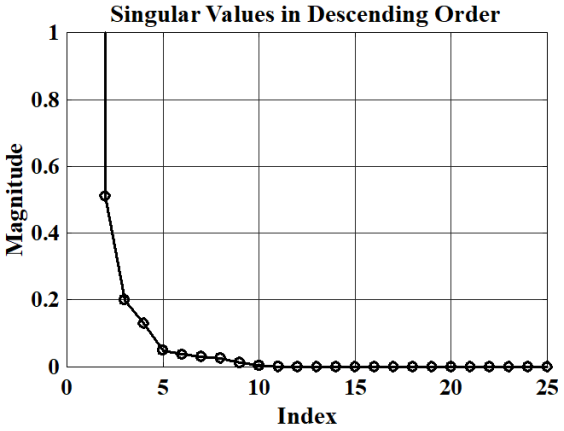

Fig. 2. Plot of singular values of a 24 mode MDM in descending order.

B. Representation of k_x and k_y outside the waveguide

This section describes how to represent the values of k_x and k_y in the MDM equation. Since it is desirable to represent the radiated far field in spherical coordinates *(r, θ, ϕ)*, we must map k_x and k_y to spherical coordinates to use in the stationary phase calculation.

The far field stationary phase approximation is well known and widely used throughout the literature [6, 11]. We repeat the equation here for convenience:

$$\underline{E}(r,\theta,\phi) \approx j\frac{ke^{-jkr}}{2\pi r}\left[\underline{\theta}_o\left\{\tilde{E}_x\cos\phi + \tilde{E}_y\sin\phi\right\} - \underline{\phi}_o\cos\theta\left(\tilde{E}_x\sin\phi + \tilde{E}_y\cos\phi\right)\right]. \quad (53)$$

Mapping k_x and k_y to spherical coordinates yields:

$$k_x = k_o\sin(\theta)\cos(\phi), \quad (54)$$

$$k_y = k_o\sin(\theta)\sin(\phi). \quad (55)$$

In order to get a hemisphere mapping of the radiated electric field in the positive propagation direction, we are interested in $-\pi/2 \le \theta \le \pi/2$ and $0 \le \phi \le \pi/2$. After substituting these values of θ and ϕ into (54, 55), we get a trajectory of k_x and k_y inside a circle of radius k_o as shown in Fig. 3 and Fig. 4.

Figure 3 shows all the k_x and k_y values obtained for ϕ=0 and $\Delta\theta$=1/L where L corresponds to the size of each quadrant in (44). The angle of ϕ is represented in Fig. 3 as the angle between the k_x and k_y axes. Since ϕ=0, all the k_x and k_y values fall on the k_y=0 axis. If we use $\phi=\pi/4$ to calculate k_x and k_y as in Fig. 4, then we see that the values of k_x and k_y fall on a trajectory that makes an angle of $\pi/4$ with the k_y=0 axis.

Note that in both Figs. 3 and 4 an equal spacing between values of θ does not result in an equal spacing in k_x and k_y. In addition, any value of k_x and k_y that falls

on the k_o radius yields a value of $|\underline{k}_T| = k_o$ which corresponds to κ=0. Any value of k_x and k_y that falls beyond the k_o radius corresponds to an imaginary value of κ. These values represent attenuating modes.

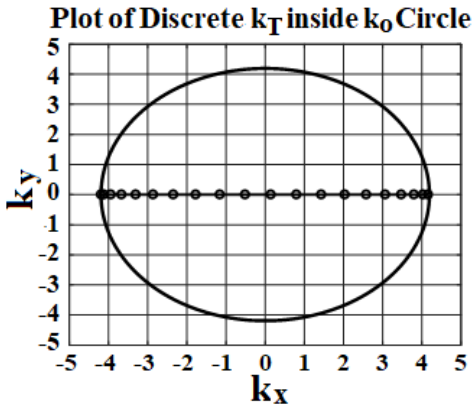

Fig. 3. Plot of k_x and k_y obtained for ϕ=0.

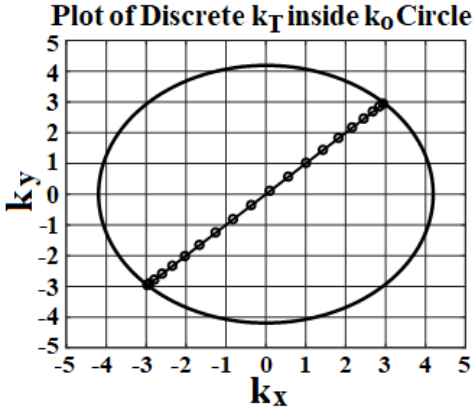

Fig. 4. Plot of k_x and k_y obtained for $\phi = \pi/4$.

IV. ANALYSIS AND COMPARISON TO SIMULATION

We compare the far field patterns and return loss at the air-interface boundary of the waveguide calculated from the MDM method to those generated using 3D EM modeling software. We performed the MDM calculations using Matlab 2017a and simulations with CST Studio Suite 2017 for comparison.

A. Computer model

The transverse dimensions of the waveguide are $\lambda_o/2$ in the $\underline{x}_o$ direction at 200 megahertz (MHz) and $\lambda_o/4$ in the $\underline{y}_o$ direction. As long as $a \geq 2b$ in Fig. 1, the dominant mode will be the TE_{10} mode [9]. The propagation of the dominant mode begins at f_c=200 MHz and the propagation of the second mode begins at $2f_c$=400 MHz. For frequencies below 200 MHz no modes will propagate in the waveguide, and for frequencies above 400 MHz more than one mode will propagate.

The distribution of the propagating TE_{10} mode generated by a matched waveguide port is a cosine distribution across the waveguide with units of volts per meter (V/m). This is the expected mode distribution for the TE_{10} mode [9]. The mode distribution peaks and is symmetric about the center of the transverse plane of the waveguide. The mode distribution does not vary in the $\underline{z}_o$ direction because it is a propagating mode.

B. MDM results and comparison

The calculations and simulations of the far field radiation patterns are determined for a frequency of 300 MHz. We chose this frequency because it stands far away from both f_c and $2f_c$. Figure 5 shows the far field patterns of E_θ and E_ϕ plotted in polar coordinates, and Fig. 6 shows the same patterns plotted in Cartesian coordinates. Figure 7 shows a calculation of the return loss based on the reflection of the TE_{10} mode at the air interface of the flanged rectangular waveguide.

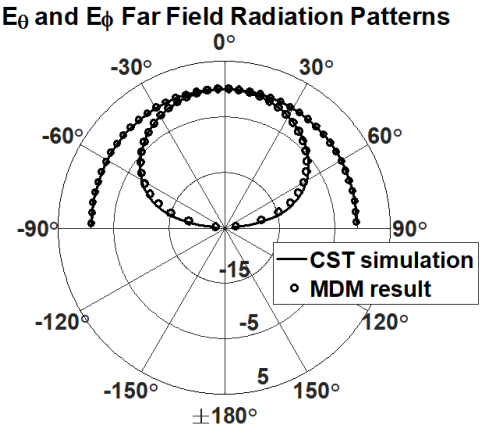

Fig. 5. Polar plot of the normalized E_θ and E_ϕ patterns.

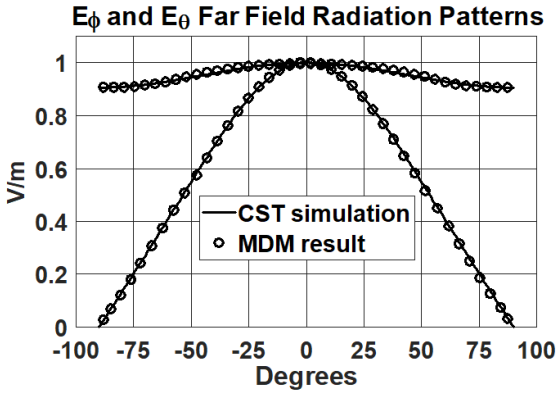

Fig. 6. Cartesian plot of the normalized E_θ and E_ϕ patterns.

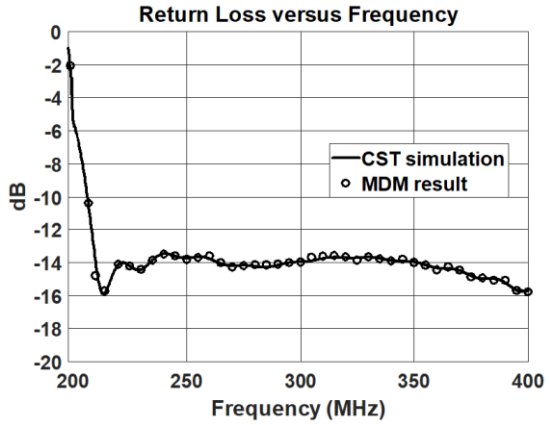

Fig. 7. Plot of return loss versus frequency for the TE_{10} mode at the waveguide air-interface boundary.

These calculations all assume an air-filled waveguide. The results show excellent agreement between the results of the MDM method and those generated by CST. In particular, the return loss at the boundary shown in Fig. 7 demonstrates the accuracy of the mode coefficients calculated using the MDM method to generate these results.

V. CONCLUSION

Traditional methods for analysis of the EM fields at the aperture of an infinitely flanged radiating rectangular waveguide require the computation of the Fourier transform of the EM fields prior to use of stationary phase. These approaches introduce additional computational costs to performing calculations of radiated far fields for this type of problem. We derive a new approach called the MDM method that allows for the direct computation EM fields at the aperture in the Fourier domain, which eliminates the need to make additional computations to obtain the Fourier transform. The result is a matrix equation that directly solves for the Fourier components needed for the far field stationary phase calculations. The results of the MDM method are in agreement with the far field radiation patterns and return loss versus frequency of an infinitely flanged radiating rectangular waveguide generated by CST. The high fidelity of agreement validates the accuracy of the less computationally expensive MDM formulation.

REFERENCES

[1] R. MacPhie and A. Zaghloul, "Radiation from a rectangular waveguide with infinite flange: Exact solution by correlation matrix," *IEEE Trans. Antennas Propagat.*, vol. AP-28, pp. 497-503, July 1980.

[2] H. Baudrand, J. Tao, and J. Atechian, "Study of radiation properties of open-ended rectangular waveguides," *IEEE Trans. Antennas Propagat.*, vol. 36, no. 8, pp. 1071-1077, Aug. 1988.

[3] H. Serizawa and K. Hongo, "Radiation for a flanged rectangular waveguide," *IEEE Trans. Antennas Propagat.*, vol. 53, no. 12, pp. 3953-3962, Dec. 2005.

[4] W. Coburn, T. Anthony, and A. Zahgloul, "Open-ended waveguide radiation characteristics – full-wave simulation versus analytical solutions," *APS International Symposium, 2010 IEEE*, 2010.

[5] C. Balanis, *Antenna Theory: Analysis and Design*. 4th ed., Hoboken, NJ: Wiley and Sons Inc., 2005.

[6] G. Mitchell and W. Wasylkiwskyj, "MDM Method for Directly Calculating the Far Field of an Open Rectangular Waveguide with an Infinite Flange," No. ARL-TR-6536, 2013.

[7] L. Felsen and N. Maruvitz, *Radiation and Scattering of Waves*. Englewood Cliffs, NJ: Prentice Hall Inc., 1973.

[8] N. Marcuvitz, *Waveguide Handbook*. New York, NY: McGraw-Hill, 1951.

[9] David Pozar, *Microwave Engineering*. 3rd ed., John Wiley and Sons, 2005.

[10] G. Strang, *Introduction to Linear Algebra*. 4th ed. Wellesley, MA: Cambridge Press, 2009.

[11] A. Ishimaru, *Electromagnetic Wave Propagation, Radiation, and Scattering*. Upper Saddle River, NJ: Prentice Hall, 1991.

Gregory A. Mitchell received his B.S. from the University of Maryland in 2005, his M.S. from The Johns Hopkins University in 2008, and his Ph.D. from The George Washington University in 2015. From 2003 to present, he has been an RF and Antenna Integration Engineer with the U.S. Army Research Laboratory. Research interests include broadband magnetic RF substrates, phased array antennas, and additive manufacturing for antennas. He is a Member of IEEE APS, ACES, and the U.S. National Committee for the International Union of Radio Science Commission A.

Wasyl Wasylkiwskyj received the B.E.E. degree from the City University of New York in1957 and the M.S. and Ph.D. degrees in Electrical Engineering from Polytechnic University, Troy, NY, in 1965 and 1968, respectively. His past research and industrial experience covers a broad spectrum of electromagnetics, including microwave components and techniques, phased array antennas, propagation and scattering, radar cross-section modeling as well as modeling of geophysical and oceanographic electromagnetic phenomena. Since 1985, he has held the position of Professor of Engineering and Applied Science at the George Washington University, Washington, DC.